Ferroptosis as a therapeutic vulnerability in MDM2 inhibition in dedifferentiated liposarcoma

CHUEH-CHUAN YEN[1-5], PAUL CHIH-HSUEH CHEN[3,4,6], SAN-CHI CHEN[2-4,7], WEN-CHI WU[2-4,7], CHIAO-HAN YEN[1,2], YUNG-CHAN LIN[1,2], PO-KUEI WU[3,4,8], CHAO-MING CHEN[3,4,8], JIR-YOU WANG[3,8,9], TA-CHUNG CHAO[2-4], MUH-HWA YANG[2,4,7] and JONATHAN A. FLETCHER[10]

[1]Department of Medical Research, Division of Clinical Research, Taipei Veterans General Hospital, Taipei 112201, Taiwan, R.O.C.; [2]Department of Oncology, Division of Medical Oncology, Center for Immuno-oncology, Taipei Veterans General Hospital, Taipei 112201, Taiwan, R.O.C.; [3]Department of Orthopedics and Traumatology, Therapeutical and Research Center of Musculoskeletal Tumor, Taipei Veterans General Hospital, Taipei 112201, Taiwan, R.O.C.; [4]School of Medicine, College of Medicine, National Yang Ming Chiao Tung University, Taipei 112304, Taiwan, R.O.C.; [5]Institute of Biopharmaceutical Sciences, College of Pharmaceutical Sciences, National Yang Ming Chiao Tung University, Taipei 112304, Taiwan, R.O.C.; [6]Department of Pathology and Laboratory Medicine, Taipei Veterans General Hospital, Taipei 112201, Taiwan, R.O.C.; [7]Institute of Clinical Medicine, College of Medicine, National Yang Ming Chiao Tung University, Taipei 112304, Taiwan, R.O.C.; [8]Department of Orthopedics and Traumatology, Taipei Veterans General Hospital, Taipei 112201, Taiwan, R.O.C.; [9]Institute of Traditional Medicine, College of Medicine, National Yang Ming Chiao Tung University, Taipei 112304, Taiwan, R.O.C.; [10]Department of Pathology, Brigham and Women's Hospital, Boston, MA 02115, USA

Received October 24, 2024; Accepted March 7, 2025

DOI: 10.3892/ol.2025.15015

Abstract. Ferroptosis is a form of necrotic cell death characterized by phospholipid oxidation. The cystine-glutamate antiporter (xCT), composed of solute carrier family 7 member 11 (SLC7A11) and SLC3A2, imports cystine for glutathione synthesis. Glutathione peroxidase 4 (GPX4) requires glutathione to counteract lipid peroxidation and prevent ferroptosis. Erastin, an xCT inhibitor, and Ras-selective lethal small molecule 3 (RSL3), a GPX4 inhibitor, suppress GPX4 function and induce ferroptosis. Tumor protein p53 (TP53) has a paradoxical role in ferroptosis regulation. Mouse double minute 2 homolog (MDM2), a negative regulator of TP53, is a key oncogene in well-differentiated liposarcoma (WDLPS) and dedifferentiated liposarcoma (DDLPS). Therefore, the present study explored the role of ferroptosis in DDLPS treatment response and resistance. Publicly available expression profiles of WDLPS, DDLPS and adipose tissue were analyzed, and the differential expression of ferroptosis-related genes regulated by the MDM2-TP53 pathway was identified in WDLPS and DDLPS. *In vitro* experiments were performed to assess the effects of erastin and RSL3 on the viability, lipid peroxidation and apoptosis of DDLPS cell lines. The results revealed that erastin and RSL3 induced lipid peroxidation and apoptosis, thereby exerting cytotoxic effects. In addition, nutlin-3, an MDM2 inhibitor, was demonstrated to increase lipid peroxidation and cytotoxicity when applied prior to erastin treatment. Notably, nutlin-3 also upregulated SLC3A2 expression in DDLPS cell lines, thereby enhancing cystine uptake. This increase in cystine uptake was suppressed by erastin. In addition, nutlin-3-induced SLC3A2 upregulation was abolished by TP53 knockdown. Nutlin-3 combined with erastin or RSL3 reduced absolute p-4EBP-1 levels in NDDLS-1 cells and p-p70S6 levels in both cell lines, with no significant impact on the p-4EBP-1/4EBP-1 and p-p70S6/p70S6 ratios. These results indicate that ferroptosis is a therapeutic vulnerability in the response to MDM2 inhibition in DDLPS. Furthermore, combining MDM2 inhibitors with ferroptosis-inducing agents may provide a potential therapeutic strategy for DDLPS and the role of mTOR in the pro-apoptotic effect of these combinations deserve further investigation.

Correspondence to: Dr Chueh-Chuan Yen, Department of Medical Research, Division of Clinical Research, Taipei Veterans General Hospital, 201, Section 2, Shih-Pai Road, Taipei 112201, Taiwan, R.O.C.
E-mail: ccyen@vghtpe.gov.tw

Dr Jonathan A. Fletcher, Department of Pathology, Brigham and Women's Hospital, 75 Francis Street, Boston, MA 02115, USA
E-mail: jfletcher@partners.org

Key words: cystine, erastin, ferroptosis, GPX4, liposarcoma, MDM2, nutlin-3, RSL3, SLC3A2, TP53, xCT

Introduction

Liposarcoma (LPS) is one of the most common types of soft tissue sarcoma (1-3). Among its four subtypes, well-differentiated LPS (WDLPS) and dedifferentiated LPS (DDLPS) share similar genomic changes, notably the amplification of the 12q13-15 chromosomal region, where mouse double minute 2 homolog (MDM2) is the primary oncogene. WDLPS rarely metastasizes and can remain stable for several years. By

contrast, DDLPS is a highly aggressive disease characterized by frequent local recurrence and distant metastasis (4). Wide surgical excision with curative intent is the preferred treatment for localized disease. However, for advanced DDLPS, despite recommended first-line chemotherapy with doxorubicin (5) and second-line options including eribulin or trabectedin (6-8), treatment outcomes remain poor.

Ferroptosis is a form of cell death characterized by the oxidative modification of phospholipid membranes, resulting in the accumulation of lipid-based reactive oxygen species (ROS) (9-11). Cysteine metabolism is crucial in the regulation of ferroptosis (9-11). The cystine-glutamate antiporter (xCT), composed of solute carrier family 7 member 11 (SLC7A11) and SLC3A2, facilitates the uptake of cystine from the extracellular environment. Once imported, cystine is reduced to cysteine, a key component of the tripeptide glutathione. Glutathione peroxidase 4 (GPX4) requires glutathione as a cofactor to reduce lipid peroxidation and prevent ferroptosis (12,13). Inactivation of GPX4, either through cystine deprivation by the xCT inhibitor erastin or direct inhibition by the GPX4 inhibitor Ras-selective lethal small molecule 3 (RSL3), leads to the accumulation of lipid-based ROS and ultimately ferroptotic cell death (13,14).

Few studies have explored the role of ferroptosis in LPS, a tumor originating from adipocytic differentiation. Tumor protein p53 (TP53), a well-known tumor suppressor mutated in nearly half of all cancers (15), plays a key role in regulating ferroptosis through multiple, sometimes paradoxical, pathways. These include suppressing SLC7A11 expression to promote ferroptosis (16); upregulating 3-hydroxy-3-methyl-glutaryl-coenzyme A reductase (HMGCR), which produces molecules with anti-ferroptotic properties (17); and inhibiting dipeptidyl-peptidase-4 (DPP4)-dependent lipid peroxidation, thereby reducing ferroptosis (18). MDM2, the key oncogene in DDLPS (19), and its homolog MDM4 (20) negatively regulate TP53 (21-24), potentially influencing ferroptotic death through both TP53-dependent and TP53-independent mechanisms (25). These findings suggest that exploring the ferroptosis pathway may lead to the discovery of novel therapeutic strategies, with MDM2 playing a critical role in the regulation of ferroptosis in DDLPS.

In the present study, an investigation of the expression of genes involved in the ferroptosis pathway in DDLPS was performed via bioinformatics, to identify differentially expressed ferroptosis-related genes. Additionally, the sensitivity of DDLPS cell lines to the ferroptosis-inducing agents erastin and RSL3 was investigated. The effects of nutlin-3, an MDM2 inhibitor, as a co- or pre-treatment with erastin or RSL3 were also investigated, and the effect of TP53 knockdown (KD) was explored.

Materials and methods

Exploration of ferroptosis-related gene expression regulated by the MDM2-TP53 pathway through bioinformatics analysis. Bioinformatics analysis was performed as previously described (26). Microarray data from the Affymetrix Human Genome U133 Plus 2.0 and Affymetrix Human Genome U133A platforms were obtained from the National Center for Biotechnology Information (NCBI) website (https://www.ncbi.nlm.nih.gov/gds/). The datasets comprised DDLPS samples from GSE21050 (U133 Plus 2.0) (27) and GSE30929 (U133A) (28), WDLPS samples from GSE20559 (U133 Plus 2.0) (29) and GSE30929 (U133A) (28), and adipose tissue samples from GSE41168 (U133 Plus 2.0) (30) and GSE35710 (U133A) (31). The gene expression data were normalized using dChip (32,33). Specific genes associated with ferroptosis were selected, and their expression levels were expressed as Z-scores following Z-score transformation.

Cell lines and reagents. DDLPS cell lines LPS853 and NDDLS-1, provided by Dr Fletcher JA (Department of Pathology, Brigham and Women's Hospital, Boston, MA 02115, USA) and Dr Ariizumi (Division of Orthopedic Surgery, Niigata University Graduate School of Medical and Dental Sciences, Niigata City, Niigata 951-8510, Japan), respectively, were used as *in vitro* models to test the efficacy of various agents. The cells were cultured in RPMI 1640 Medium (Gibco; Thermo Fisher Scientific, Inc.) supplemented with Fetal Bovine Serum (Corning, Inc.) and Penicillin-Streptomycin (Gibco; Thermo Fisher Scientific, Inc.) and incubated at 37˚C with 5% CO_2. The xCT inhibitor erastin (CAS no. 571203-78-6; Cayman Chemical Company), GPX4 inhibitor RSL3 (CAS no. 1219810-16-8; Cayman Chemical Company) and HMGCR inhibitors lovastatin (S2061; Selleck Chemicals) and simvastatin (S1792; Selleck Chemicals) were evaluated for their ferroptosis-inducing effects. Nutlin-3a (S8059; Selleck Chemicals) was used as an MDM2 antagonist; this is the active enantiomer of nutlin-3, and for simplicity is referred to as nutlin-3 throughout the manuscript. Ferrostatin-1 (Fer-1; CAS no. 347174-05-4; Cayman Chemical Company) was used to inhibit ferroptosis. The antibodies used for immunoblotting were as follows: p53 (cat. no. 2527S; 1:1,000; Cell Signaling Technology, Inc.), MDM2 (cat. no. 86934S; 1:1,000; Cell Signaling Technology, Inc.), SLC7A11 (cat. no. A13685; 1:1,000; ABclonal Biotech Co., Ltd.), GPX4 (cat. no. A1933; 1:1,000; ABclonal Biotech Co., Ltd.), SLC3A2/CD98hc (cat. no. A3658; 1:1,000; ABclonal Biotech Co., Ltd.), 4EBP1 (cat. no. 9644; 1:1,000; Cell Signaling Technology, Inc.), phosphorylated (p)-4EBP1 (cat. no. 9459; 1:1,000; Cell Signaling Technology, Inc.), p70S6 (cat. no. 9202; 1:1,000; Cell Signaling Technology, Inc.), p-p70S6 (cat. no. 9205; 1:1,000; Cell Signaling Technology, Inc.) and β-actin (cat. no. ab6276; 1:1,000; Abcam).

Lipid peroxidation assay. The DDLPS cell lines ($2.5x10^5$ cells/well) were seeded in six-well plates and incubated at 37˚C with different concentrations of test agents for specific durations. For single agent treatment, cells were treated with erastin (12 μM for NDDLS-1, 20 μM for LPS853), RSL3 (0.2 μM for both), lovastatin (18 μM for both), or simvastatin (18 μM for both) for 24 h. For combination with Fer-1, cells were treated with erastin (8 μM for LPS853, 20 μM for NDDLS-1), or RSL3 (0.05 μM for both), and combined with Fer-1 (4, 6, or 8 μM), with co-treatment of erastin and Fer-1 for 48 h and RSL3 and Fer-1 for 4 h. For combination with nutlin-3, cells were treated with erastin (8 or 16 μM for LPS853, 12 or 20 μM for NDDLS-1), or RSL3 (0.2 or 0.4 μM for both), and combined with nutlin-3 (10 μM for both). Co-treatment

with erastin and nutlin-3 or RSL3 and nutlin-3 was performed for 24 h, whereas in the sequential treatment, cells were first exposed to nutlin-3 for 24 h, followed by treatment with either erastin or RSL3 for an additional 24 h. After treatment, cells were incubated with 2 μM BODIPY 581/591 C11 (Thermo Fisher Scientific, Inc.) for 30 min at 37˚C. After this, the cells were collected, resuspended in 500 μl phosphate-buffered saline (PBS), and analyzed using a BD FACSCanto™ II flow cytometry system (BD Biosciences) (34). Data were analyzed using FlowJo software (version 7.6; FlowJo LLC). The experiment was performed in triplicate.

Cell viability assay. Cell viability was assessed using the Cell Counting Kit-8 (CCK-8) assay (Abbkine Scientific Co., Ltd.) according to the manufacturer's instructions. In brief, cells were plated in 96-well plates at a concentration of 5,000 cells in 100 μl/well. The following day, different concentrations of the test agents were added to individual wells and incubated at 37˚C for the appropriate duration. The treatment conditions were as follows: for single agent treatment, Erastin (4, 8, 12, 16, 20 μM), RSL3 (1, 2, 3, 4, 5 μM), lovastatin (6, 12, 18, 24, 30 μM), or simvastatin (6, 12, 18, 24, 30 μM) was used for 24-h treatment; for combination with Fer-1, Erastin (3, 6, 9, 12, 15 μM) or RSL3 (0.01, 0.02, 0.03, 0.04, 0.05 μM) were combined with Fer-1 (1, 2, 3, 4, 5 μM) for 48-h treatment; for combination with nutlin-3, Erastin (3, 6, 9, 12, 15 μM) or RSL3 (0.01, 0.02, 0.03, 0.04, 0.05 μM) were combined with nutlin-3 (4, 8, 12, 16, 20 μM). Co-treatment with erastin and nutlin-3 or RSL3 and nutlin-3 was performed for 24 h, whereas in the sequential treatment, cells were first exposed to nutlin-3 for 24 h, followed by treatment with either erastin or RSL3 for an additional 24 h. After incubation, 10 μl CCK-8 solution was added to each well, followed by incubation for 1.5-2 h. The absorbance at 450 nm was measured for each well using a microplate reader. The combination index (CI) for two-drug combinations was calculated using CalcuSyn software (Biosoft), where CI <1, CI=1 and CI >1 indicate synergism, additivity and antagonism, respectively. All experiments were performed in triplicate (35).

Apoptosis assessment. Apoptosis was assessed as previously described (26). Specifically, for single agent treatment, cells ($1x10^5$ cells/well) were treated with erastin (2, 4, 6, 8 μM for LPS853, 3, 6, 9, 12 μM for NDDLS-1) or RSL3 (0.1, 0.2, 0.3, 0.4 μM for both), with LPS853 cells exposed to erastin for 24 h, NDDLS-1 cells exposed to erastin for 48 h, and both cell lines treated with RSL3 for 24 h. For combination with nutlin-3, cells ($1x10^5$ cells/well) were treated with erastin (10 μM), or RSL3 (0.4 μM), and combined with nutlin-3 (10 μM). Co-treatment with erastin and nutlin-3 or RSL3 and nutlin-3 was performed for 24 h, whereas in the sequential treatment, cells were first exposed to nutlin-3 for 24 h, followed by treatment with either erastin or RSL3 for an additional 24 h. After treatment, cells were washed with 1X PBS and resuspended in 100 μl staining solution containing annexin V-fluorescein isothiocyanate and propidium iodide in HEPES buffer (BD Pharmingen). The cells were incubated at room temperature for 15 min, then diluted in 1X annexin V-binding buffer (BD Pharmingen) and analyzed by flow cytometry with a BD FACSCanto II system, BD FACSDiva Software v8.0.2 operating software (all BD Biosciences) and FlowJo (version 7.6; FlowJo LLC) analysis software. The experiment was performed in triplicate.

Immunoblotting. Immunoblotting was performed as previously described (36). Cells were treated with erastin (8 μM), RSL3 (0.2 μM), or nutlin-3 (12 μM), either as single agent or various combinations, for 24 h. After treatment, cultured monolayer cells were rinsed with PBS and lysed using RIPA Lysis and Extraction Buffer (Thermo Fisher Scientific, Inc.). The cell suspensions were then incubated at 4˚C for 30 min, followed by centrifugation at 15,974 x g for 30 min at 4˚C. Total protein concentrations were measured using the Pierce BCA Protein Assay Kit (Thermo Fisher Scientific, Inc.). Proteins (50 μg per lane) were separated by 12% sodium dodecyl sulfate-polyacrylamide gel electrophoresis (SDS-PAGE) and transferred to polyvinylidene difluoride (PVDF) membranes (PerkinElmer, Inc.). The membranes were blocked with 5% bovine serum albumin (BSA; Bionovas Biotechnology Co., Ltd.) at room temperature for 30 min. Primary antibodies were incubated at 4˚C overnight, while secondary antibodies were incubated at room temperature for 45 min. Primary and secondary antibodies were prepared in 5% bovine serum albumin (BSA). The secondary antibodies, Anti-rabbit IgG (cat. no. 7074S) and Anti-mouse IgG (cat. no. 7076S), were diluted at 1:4,500 and purchased from Cell Signaling Technology, Inc. The immunoreactive bands were visualized using Immobilon Western Chemiluminescent HRP Substrate (MilliporeSigma) and a UVP ChemStudio PLUS Touch Western Blot Imaging System (Analytik Jena AG). Densitometric analysis was performed using ImageJ software (version 1.51, National Institutes of Health).

Cystine uptake assay. Cystine uptake was measured using a Cystine Uptake Assay Kit (Dojindo Laboratories, Inc.) according to the manufacturer's instructions. Cells ($1x10^4$ cells/well) were seeded in a black 96-well plate for 24 h. The medium was then replaced and cells were treated with single agent erastin (40 μM) or nutlin-3 (10 μM) or combination for the time period specified by the manufacturer. After treatment,, the culture medium was aspirated, and the cells were washed three times with serum-free RPMI 1640 prior to incubation in serum-free RPMI 1640 for 5 min at 37˚C. Subsequently, the cells were incubated with Cystine Analog Solution (selenocystine) from the kit in serum-free RPMI 1640 for 30 min at 37˚C. Fluorescence was measured using a fluorescence microplate reader with an excitation wavelength of 490 nm and an emission wavelength of 535 nm.

Small interfering RNA (siRNA)-mediated knockdown (KD) of TP53. The TP53 KD experiment was conducted using the ON-TARGETplus system (Horizon Discovery, Ltd.). Cells ($1x10^6$) were first treated with DharmaFECT 1 Transfection Reagent (cat. no. T-2001-03; GE Healthcare Dharmacon, Inc.; ON-TARGETplus system) and subsequently transfected with ON-TARGETplus Human TP53 (cat. no. 7157) siRNA-SMARTpool (cat. no. L-003329-00-0005) target sequences: GAAAUUUGCGUGUGGAGUA, GUGCAGCUG UGGGUUGAUU, GCAGUCAGAUCCUAGCGUC and GGA GAAUAUUUCACCCUUC; 20 μM) or the ON-TARGETplus Non-targeting Pool (cat. no. D-001810-10-20; GE Healthcare Dharmacon, Inc.) target sequences: UGGUUUACAUGU

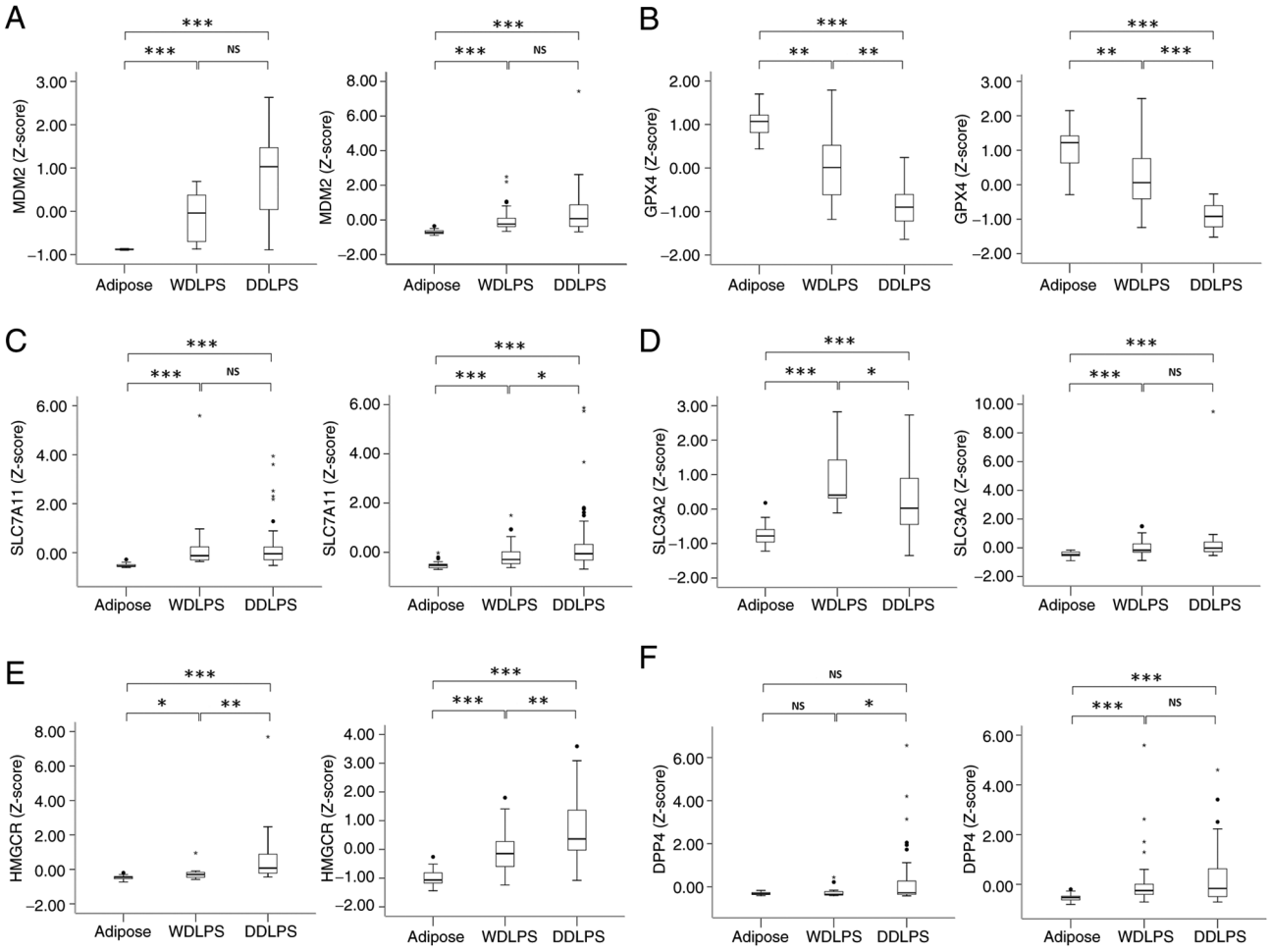

Figure 1. Comparison of the expression levels of six ferroptosis-related genes among adipose, WDLPS and DDLPS tissues. Expression levels of (A) MDM2, (B) GPX4, (C) SLC7A11, (D) SLC3A2, (E) HMGCR and (F) DPP4. In each panel, data in the left graph are from GSE21050, GSE20559 and GSE41168 (U133 Plus 2.0) and data in the right graph are from GSE30929 and GSE35710 (U133A). *P<0.05, **P<0.01 and ***P<0.001 as indicated. Differences in levels among the different tissue types were analyzed using Kruskal-Wallis followed by Dunn's post hoc test. NS, not significant; WDLPS, well-differentiated liposarcoma; DDLPS, dedifferentiated liposarcoma; MDM2, mouse double minute 2 homolog; GPX4, glutathione peroxidase 4; SLC7A11, solute carrier family 7 member 11; SLC3A2, solute carrier family 3 member 2; HMGCR, 3-hydroxy-3-methyl-glutaryl-coenzyme A reductase; DPP4, dipeptidyl peptidase-4.

CGACUAA, UGGUUUACAUGUUGUGUGA, UGGUUUACAUGUUUUCUGA, and UGGUUUACAUGUUUUCCUA; 20 μM as a negative control. However, the sense and antisense strand sequences were not provided for either siRNA. Following transfection, cells were incubated at 37˚C for 48 h.

The KD efficiency of TP53 was confirmed by reverse transcription-quantitative PCR (RT-qPCR). RNA extraction was performed using the LabPrep™ RNA Plus Mini Kit (LabPrep). RT was carried out using the HiScript™ First Strand cDNA Synthesis Kit (Bionovas Biotechnology Co., Ltd.) according to the manufacturer's protocol. qPCR was performed using SYBR Green PCR Master Mix (Thermo Fisher Scientific, Inc.) with the following primers: TP53 forward, 5'-GCCATCTACAAGCAGTCACAG-3' and reverse, 5'-TCATCCAAATACTCCACACGC-3'; GAPDH forward, 5'-GCCAAGGTCATCCATGACAACT-3' and reverse, 5'-GAGGGGCCATCCACAGTCTT-3'. The thermocycling conditions were as follows: 95˚C for 10 min, followed by 36 cycles of 95˚C for 15 sec and 55˚C for 60 sec. Amplification and analysis were performed using the QuantStudio3 Real-Time PCR System (Applied Biosystems; Thermo Fisher Scientific, Inc.). Gene copy numbers were calculated according to the $2^{-\Delta\Delta Cq}$ method (37).

Statistical analysis. Differences in the expression of genes among the DDLPS, WDLPS and adipose tissues were analyzed using the Kruskal-Wallis test, followed by Dunn's post hoc test for pairwise comparisons. In the cell-based experiments, differences between two groups were analyzed using unpaired Student's t-test and among multiple groups were analyzed by one-way ANOVA followed by Bonferroni's post hoc test. P<0.05 was considered to indicate a statistically significant difference. Statistical analysis was conducted using SPSS Statistics for Windows, version 17.0 (SPSS Inc.).

Results

Ferroptosis-related genes regulated by the MDM2-TP53 pathway are differentially expressed in DDLPS. Publicly available data were analyzed to identify potential differences in the expression of ferroptosis-related genes regulated by the MDM2-TP53 pathway. The expression levels of MDM2 were significantly upregulated in WDLPS and DDLPS compared with those in adipose tissue (Fig. 1A). By contrast, the GPX4 expression levels in DDLPS were significantly lower than those in both adipose tissue and WDLPS (Fig. 1B), which

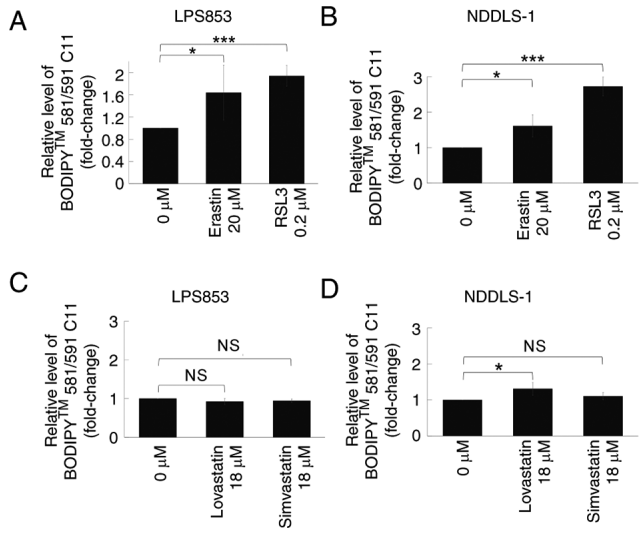

Figure 2. Effect of various treatments on lipid peroxidation levels in dedifferentiated liposarcoma cell lines. Effect on lipid peroxidation levels of treatment with erastin or RSL3 in (A) LPS858 and (B) NDDLS-1 cells or treatment with lovastatin or simvastatin in (C) LPS858 and (D) NDDLS-1 cells, determined by flow cytometry. Results are presented as the mean ± standard error of the mean from three independent experiments. *P<0.05 and ***P<0.001 as indicated. RSL3, Ras-selective lethal small molecule 3; NS, not significant.

may contribute to a pro-ferroptosis phenotype. The expression levels of HMGCR observed in DDLPS were higher compared with those in adipose tissue and WDLPS (Fig. 1E), potentially contributing to an anti-ferroptosis effect. The expression levels of SLC7A11 and SLC3A2 were higher in both types of LPS compared with those in adipose tissue. However, the differential expression of DPP4 in adipose tissue, WDLPS and DDLPS was inconsistent between the two platforms (Fig. 1C, D and F).

DDLPS cell lines show variable sensitivity to ferroptosis-inducing agents. The potential lipid peroxidation effects of ferroptosis-inducing agents on two DDLPS cell lines were evaluated. Both erastin and RSL3 treatment significantly increased lipid peroxidation levels in both cell lines compared with those in untreated cells, as demonstrated by flow cytometry (Figs. 2 and S1). However, regarding the two statins with HMGCR inhibitory activity, only lovastatin exhibited a significant effect, inducing an increase in lipid peroxidation levels in NDDLS-1 cells only. The cytotoxic effects of these four agents were then assessed in the two cell lines. Erastin and RSL3 exerted significant cytotoxic effects on both DDLPS cell lines at relatively low doses (Fig. 3A and B). Lovastatin and simvastatin also showed significant, although less potent, efficacy against the two DDLPS cell lines (Fig. 3C and D). In addition, erastin (Figs. 3E and G, S2A and C) and RSL3 (Figs. 3F and H, S2B and D) induced apoptosis in both DDLPS cell lines. On the basis of these results, only erastin and RSL3 were used in subsequent experiments.

Erastin and RSL3 exert cytotoxic effects primarily through ferroptosis. Further analysis was performed to determine whether ferroptosis is the primary mechanism underlying the cytotoxic effects of erastin and RSL3. The ferroptosis inhibitor Fer-1 partially diminished the lipid peroxidation induced by erastin or RSL3 in the LPS853 and NDDLS-1 cell lines (Figs. 4A-D and S3). Furthermore, CCK-8 assay results revealed that Fer-1 attenuated the cytotoxic effects of both erastin and RSL3 in both DDLPS cell lines (Fig. 4E-H). These results indicate that both erastin and RSL3 exert their cytotoxic effects at least in part via the induction of ferroptosis.

Treatment sequence is crucial for the synergy of nutlin-3 with erastin but not RSL3 in ferroptosis induction and cytotoxicity. The potential synergistic effects of combining nutlin-3 with erastin or RSL3 were evaluated. First, their effects on lipid peroxidation were tested. Co-treatment with nutlin-3 and erastin (Figs. 5A and C, S4A and C) did not significantly alter the extent of lipid peroxidation compared with that induced by erastin alone in either DDLPS cell line. However, pre-treatment with nutlin-3 for 24 h significantly increased the lipid peroxidation-inducing effects of erastin in both DDLPS cell lines (Figs. 5B and D, S4B and D). By contrast, whether nutlin-3 and RSL3 were co-administered or applied sequentially did not clearly impact the lipid peroxidation-inducing effects in either DDLPS cell line (Figs. 5E-H and S4E-H).

The synergistic cytotoxic effects of nutlin-3 combined with erastin or RSL3 were evaluated using the CCK-8 assay. Co-treatment with nutlin-3 and erastin did not exhibit a significant synergy in cytotoxicity (Fig. 6A and C). However, a 24-h pre-treatment with nutlin-3 followed by treatment with erastin synergistically induced cytotoxicity in both DDLPS cell lines (Fig. 6B and D). For nutlin-3 combined with RSL3, the treatment sequence affected the synergy of the cytotoxicity in LPS853 cells (Fig. 6E and F) but not in NDDSL-1 cells (Fig. 6G and H). Similarly, in the apoptosis assay, the apoptosis-inducing effects of nutlin-3 and erastin varied according to the treatment sequence (Figs. 7A-D, S5A and B, S6A and B), whereas those of nutlin-3 and RSL3 did not (Figs. 7E-H, S5C and D, S6C and D). These findings indicate that nutlin-3 pre-treatment significantly enhances the ferroptosis-inducing and cytotoxic effects of erastin but not those of RSL3.

Nutlin-3-induced upregulation of SLC3A2 and cystine uptake in DDLPS cell lines is suppressed by erastin. As shown in Fig. 8A and D, nutlin-3 treatment increased the expression of MDM2 and TP53. This is consistent with previous studies which have shown that nutlin-3 disrupts the interaction between MDM2 and TP53, prevents their ubiquitination and leads to increased expression of both proteins (38-40). Nutlin-3 treatment also increased the expression of SLC3A2 (Fig. 8B and E), while its effects on SLC7A11 and GPX4 expression were inconsistent between the two cell lines. In the cystine uptake assay, nutlin-3 treatment significantly increased the uptake of a selenocystine fluorescent probe, and this effect was significantly suppressed by erastin (Fig. 8C and F). This suggests that nutlin-3 treatment increased the expression of SLC3A2 in DDLPS, leading to enhanced cystine uptake and greater sensitivity to erastin. This may explain why nutlin-3 pre-treatment synergistically promoted the cytotoxic effects of erastin but not those of RSL3.

Nutlin-3-induced SLC3A2 upregulation is abolished by TP53 KD. The mechanism by which nutlin-3 induces SLC3A2 upregulation was investigated. Given the role of TP53 in the regulation of SLC3A2 expression, TP53 KD experiments

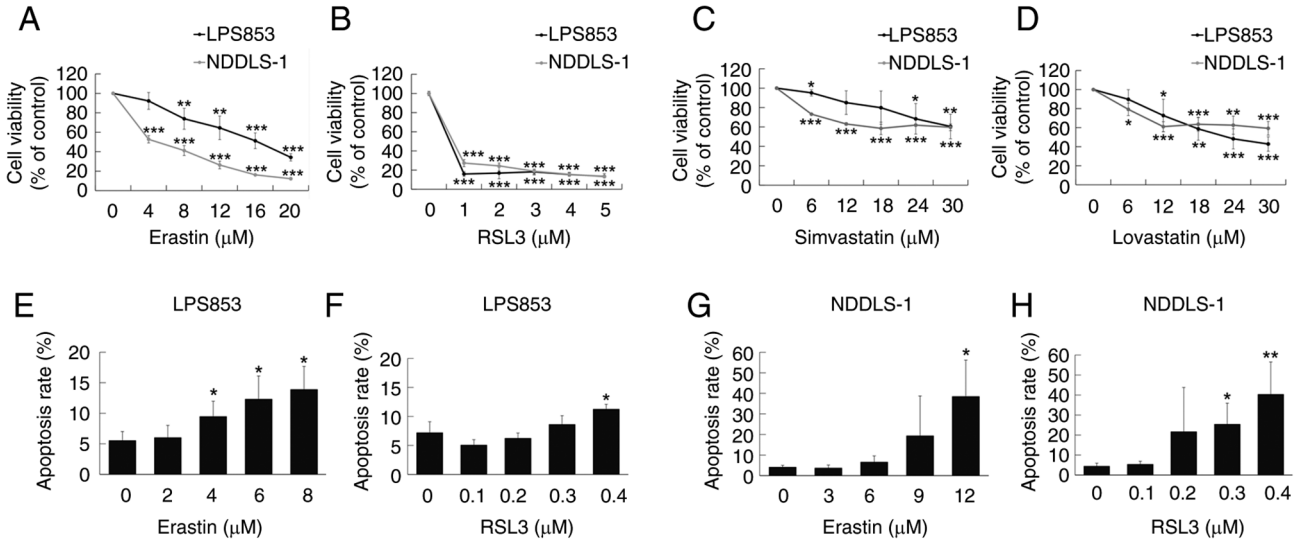

Figure 3. Effect of various treatments on the cell viability and apoptosis of two dedifferentiated liposarcoma cell lines. Cell viability was measured by Cell Counting Kit-8 assay after treatment with (A) erastin, (B) RSL3, (C) simvastatin or (D) lovastatin. Apoptosis was assessed through annexin V and PI staining following treatment with (E) erastin or (F) RSL3 in LPS853 cells and (G) erastin or (H) RSL3 in NDDLS-1 cells. Results are presented as the mean ± standard error of the mean from three independent experiments. *P<0.05, **P<0.01 and ***P<0.001 vs. control (0 μM).

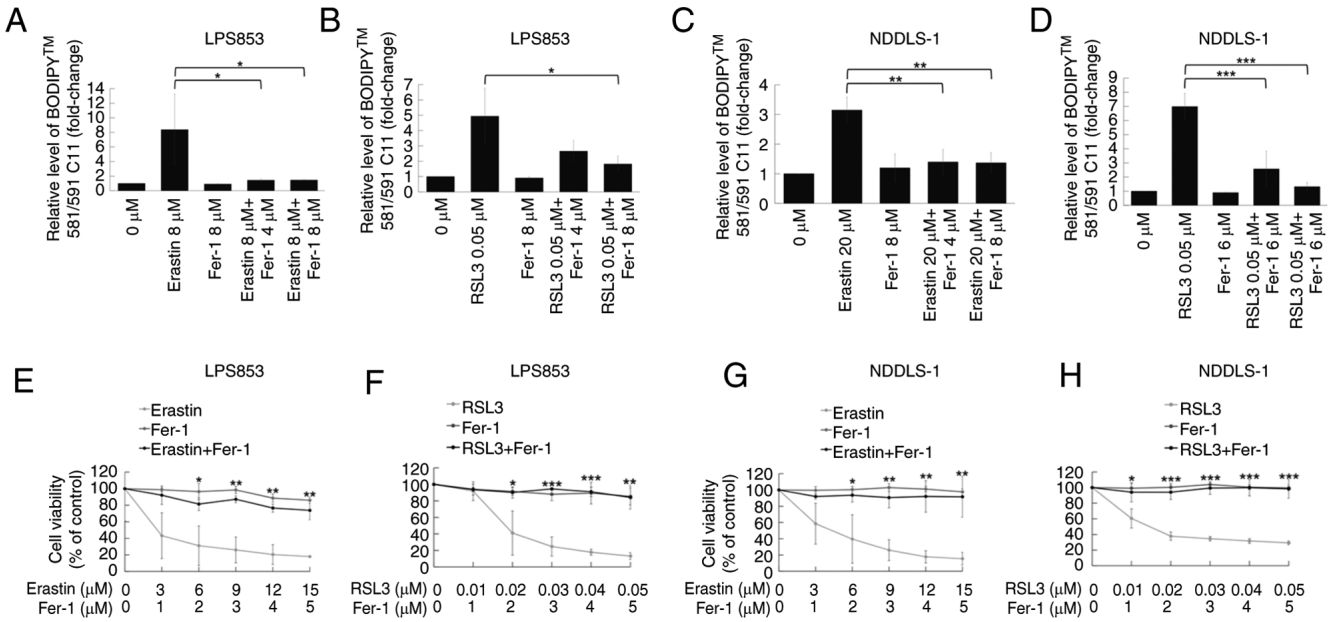

Figure 4. Effect of Fer-1 on the lipid peroxidation and viability of dedifferentiated liposarcoma cell lines treated with erastin or RSL3. Lipid peroxidation levels, determined by flow cytometry, in LPS853 cells treated with (A) erastin or (B) RSL3 or in NDDLS-1 cells treated with (C) erastin or (D) RSL3, with or without Fer-1. Cell viability, measured by Cell Counting Kit-8 assay in LPS853 cells after treatment with (E) erastin or (F) RSL3 or in NDDLS-1 cells treated with (G) erastin or (H) RSL3, with or without Fer-1. Results are presented as the mean ± standard error of the mean from three independent experiments. *P<0.05, **P<0.01 and ***P<0.001 vs. single agent erastin or RSL3. Fer-1, ferrostatin 1.

were performed. As shown in Fig. 9, the nutlin-3-induced SLC3A2 upregulation previously observed in the untransfected DDLPS cell lines was abolished by TP53 KD. This result highlights the critical role of TP53 in nutlin-3-induced SLC3A2 upregulation.

Combination of nutlin-3 with erastin or RSL3 suppresses the mTOR pathway. Notably, the present study found that the combination of nutlin-3 with either erastin or RSL3 can increase apoptosis. The mTOR pathway has been reported to play a role in the regulation of ferroptosis (41-43). In addition, inhibition of mTOR pathway is known to induce apoptosis (44-46). Therefore, the involvement of this pathway was assessed via the evaluation of the mTOR downstream effectors eukaryotic translation initiation factor 4E binding protein 1 (4EBP1) and p70 ribosomal protein S6 kinase (p70S6) in DDLPS cells using western blotting. As shown in Fig. 10, the combination of nutlin-3 with erastin or RSL3 suppressed the absolute p-4EBP1 levels in NDDLS-1 cells and p-p70S6 levels in both cell lines.

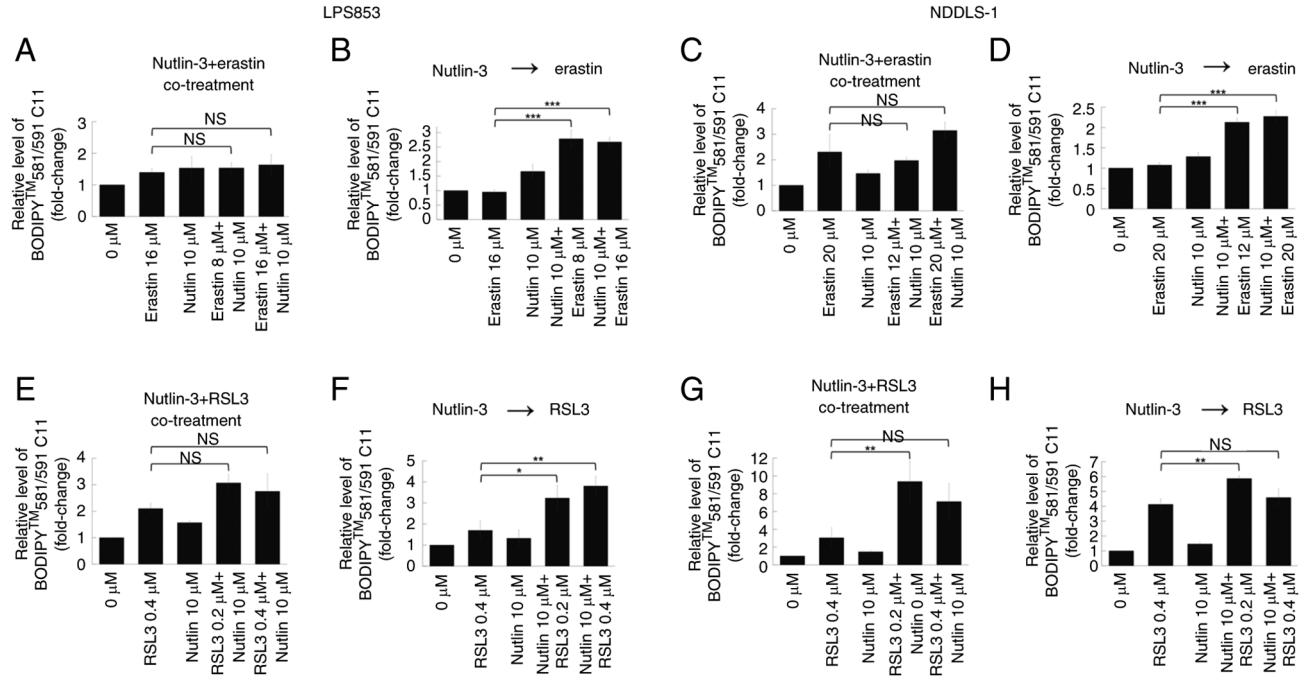

Figure 5. Effect of nutlin-3 co- or pre-treatment with erastin or RSL3 on lipid peroxidation in dedifferentiated liposarcoma cell lines, as determined by flow cytometry. Lipid peroxidation induced by nutlin-3 and erastin (A) as a co-treatment or (B) sequentially in LPS853 cells, and (C) as a co-treatment or (D) sequentially in NDDLS-1 cells. Lipid peroxidation induced by nutlin-3 and RSL3 (E) as a co-treatment or (F) sequentially in LPS853 cells, and (G) as a co-treatment or (H) sequentially in NDDLS-1 cells. In the sequential treatment, the arrow indicates that the cells were exposed to nutlin-3 for 24 h prior to treatment with erastin. Results are presented as the mean ± standard error of the mean from three independent experiments. *P<0.05, **P<0.01 and ***P<0.001 as indicated. NS, not significant.

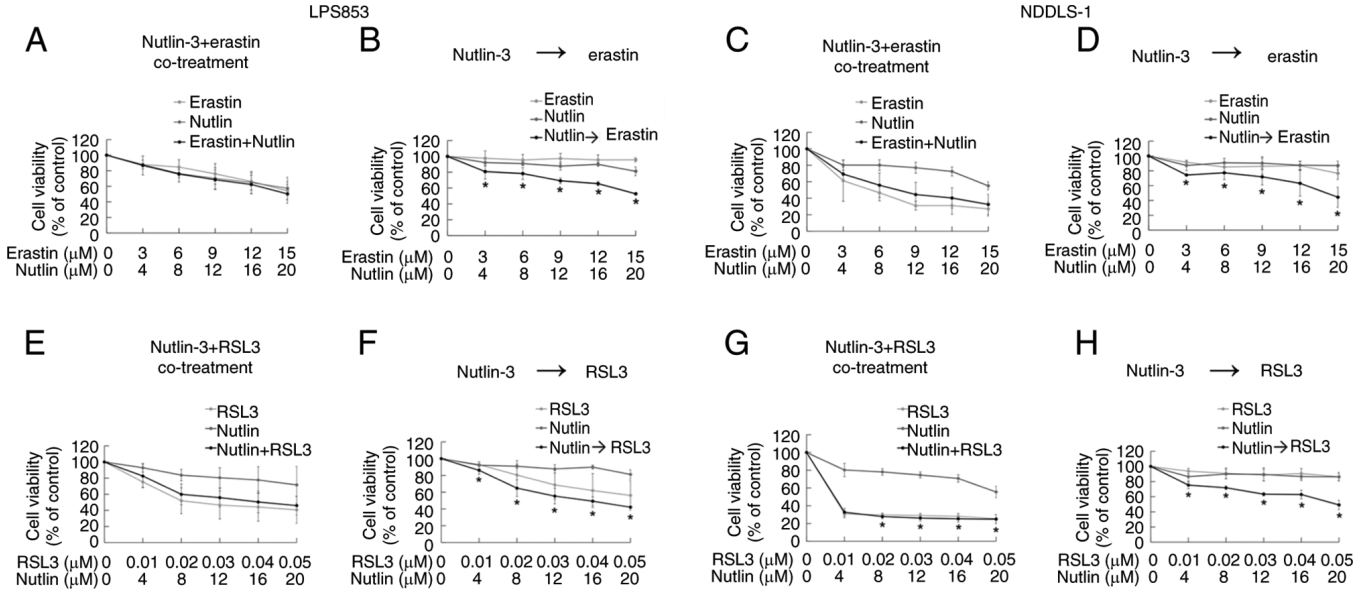

Figure 6. Effect of nutlin-3 co- or pre-treatment with erastin or RSL3 on the viability of dedifferentiated liposarcoma cell lines, measured by Cell Counting Kit-8 assay. Viability of LPS853 cells treated with nutlin-3 and erastin (A) as a co-treatment or (B) sequentially, and of NDDLS-1 cells treated with these agents (C) as a co-treatment or (D) sequentially. Viability of LPS853 cells treated with nutlin-3 and RSL3 (E) as a co-treatment or (F) sequentially, and NDDLS-1 cells treated with these agents (G) as a co-treatment or (H) sequentially. In the sequential treatment, the arrow indicates that the cells were exposed to nutlin-3 prior to treatment with erastin. Results are presented as the mean ± standard error of the mean from three independent experiments. *Combination index <1.

However, these treatment combinations had no significant effect on the p-4EBP1/4EBP1 and p-p70S6/p70S6 ratios. This suppression of the mTOR pathway may contribute to the apoptosis-inducing effects observed with these combinations, but more studies are needed for clarity.

Discussion

In the present study, bioinformatics analysis identified that several ferroptosis-related genes are differentially expressed in DDLPS. Additionally, *in vitro* experiments demonstrated that

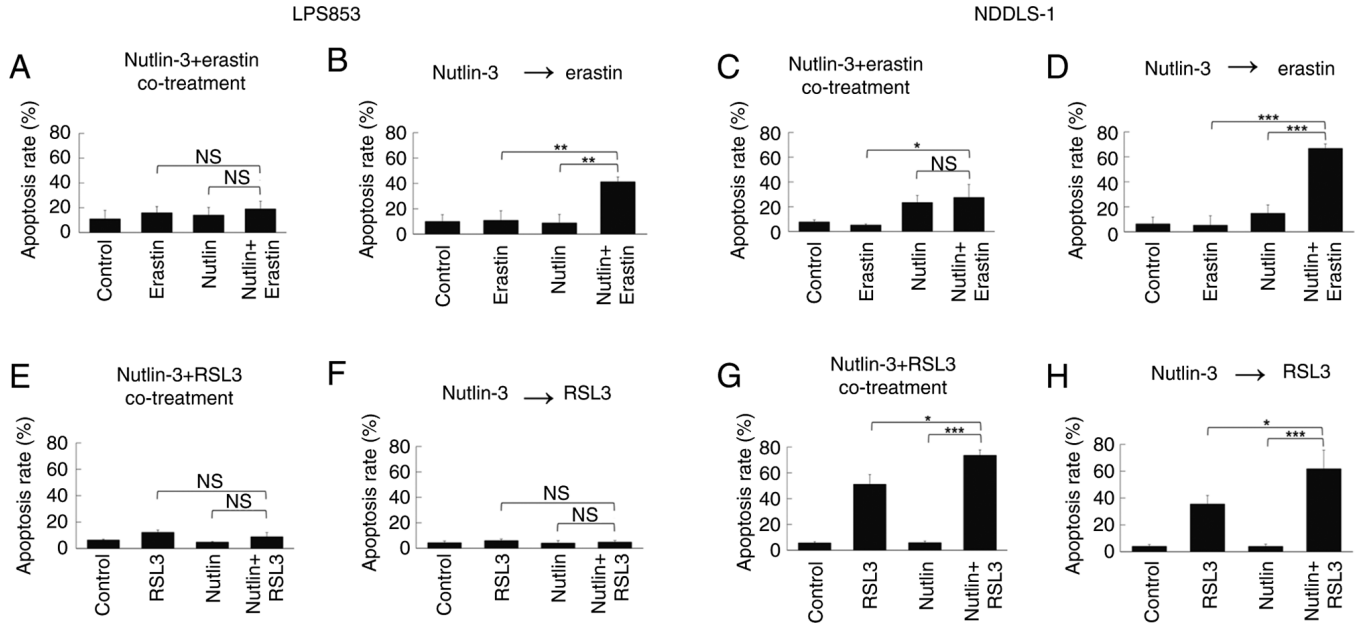

Figure 7. Effect of nutlin-3 co- or pre-treatment with erastin or RSL3 on the apoptosis of dedifferentiated liposarcoma cell lines, measured by annexin V and PI staining. Apoptosis of LPS853 cells treated with nutlin-3 and erastin (A) as a co-treatment or (B) sequentially, and NDDLS-1 cells treated with these agents (C) as a co-treatment or (D) sequentially. Apoptosis of LPS853 cells treated with nutlin-3 and RSL3 (E) as a co-treatment or (F) sequentially, and of NDDLS-1 cells treated with these agents (G) as a co-treatment or (H) sequentially. In the sequential treatment, the arrow indicates that the cells were exposed to nutlin-3 for 24 h prior to treatment with erastin. Results are presented as the mean ± standard error of the mean from three independent experiments. *P<0.05, **P<0.01 and ***P<0.001 as indicated. NS, not significant.

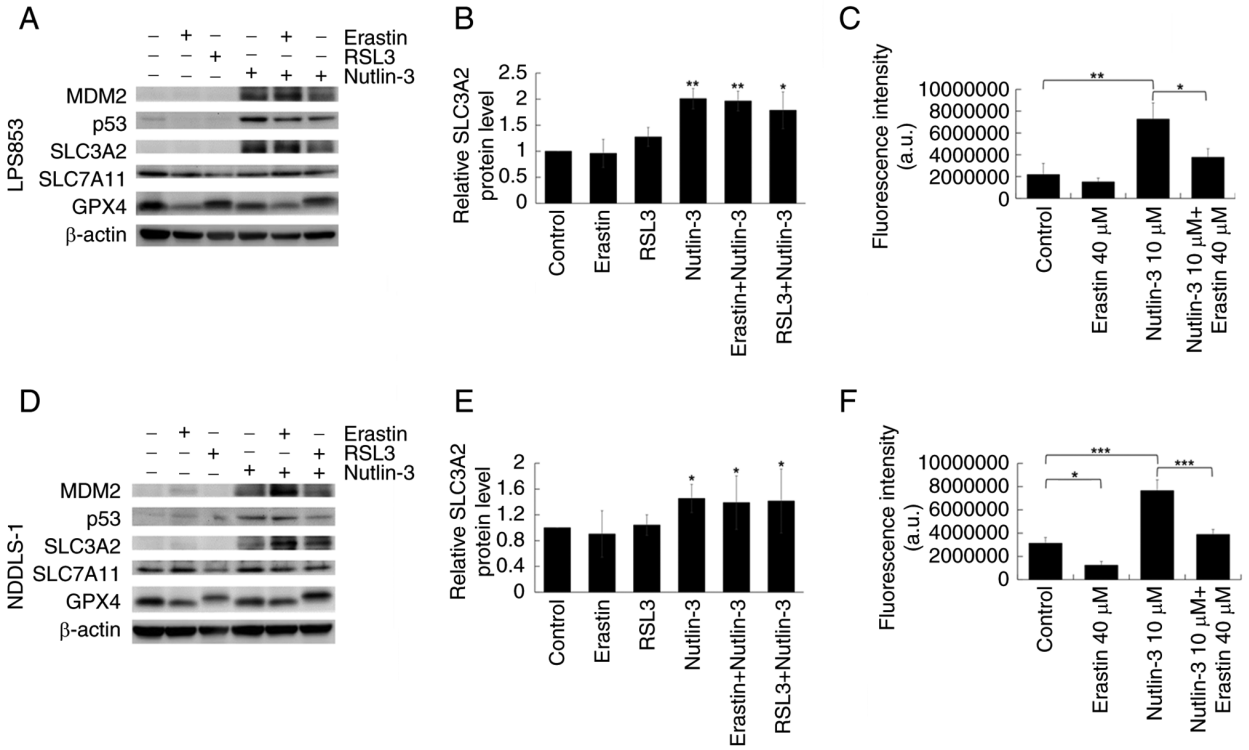

Figure 8. Immunoblotting of dedifferentiated liposarcoma cell lines following treatment with either erastin or RSL3 alone or with nutlin-3 pre-treatment and cystine uptake assay of these cell lines following treatment with either single agent erastin or nutlin-3 or combination. (A) Representative western blots, (B) quantification of SLC3A2 expression and (C) cystine uptake in LPS853 cells. (D) Representative western blots, (E) quantification of SLC3A2 expression and (F) cystine uptake in NDDLS-1 cells. Results are presented as the mean ± standard error of the mean from three independent experiments. *P<0.05, **P<0.01 and ***P<0.001 vs. control (0 μM) or as indicated.

two DDLPS cell lines were sensitive to ferroptosis-inducing agents, particularly erastin and RSL3. Furthermore, treatment of the cells with nutlin-3, an MDM2 inhibitor, followed by erastin, resulted in increased ferroptosis-inducing and

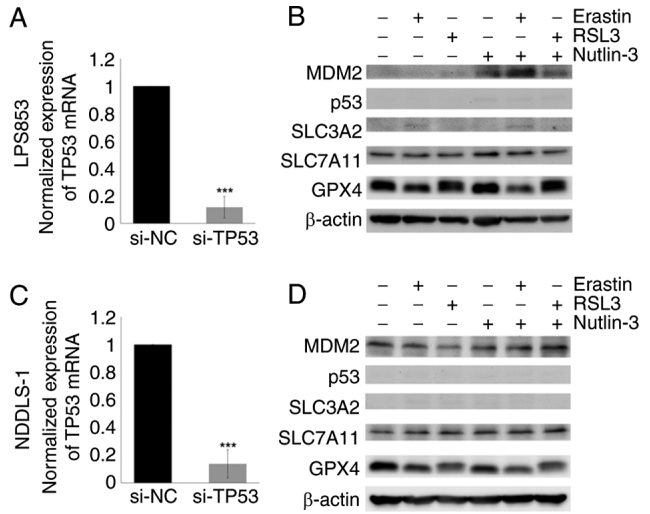

Figure 9. Immunoblotting of ferroptosis-related proteins in dedifferentiated liposarcoma cell lines following transfection with TP53 siRNA and treatment with erastin or RSL3, alone or with nutlin-3 pre-treatment. (A) Transfection success of TP53 siRNA and (B) the effects of erastin, RSL3 and/or nutlin-3 in LPS853 cells with TP53 knockdown. (C) Transfection success of TP53 siRNA and (D) the effects of erastin, RSL3 and/or nutlin-3 in NDDLS-1 cells with TP53 knockdown. Results are presented as the mean ± standard error of the mean from three independent experiments. ***P<0.001 vs. control. si-NC, transfection with non-target control siRNA; si-TP53, transfection with TP53 siRNA.

cytotoxic effects. Nutlin-3 also upregulated the expression of SLC3A2 in the DDLPS cell lines, which increased cystine uptake, and erastin attenuated these effects. TP53 KD diminished the effect of nutlin-3 on SLC3A2, indicating that TP53 contributes to SLC3A2 upregulation. Combining nutlin-3 with either of these ferroptosis-inducing agents reduced the absolute p-4EBP1 levels in NDDLS-1 cells and p-p70S6 levels in both cell lines, without significantly affecting the p-4EBP1/4EBP1 and p-p70S6/p70S6 ratios. This suggests a potential role of the mTOR pathway in the pro-apoptotic effect of these combinations, which warrants further investigation.

MDM2 and CDK4 are oncogenes located in the 12q13-15 amplified chromosomal regions in both WDLPS and DDLPS (47). CDK4 phosphorylates Rb, promoting cell cycle progression (48), while MDM2 suppresses the function of TP53 by downregulating its expression, exporting it from the nucleus to the cytoplasm, and cooperating with MDM4 to induce TP53 polyubiquitination and subsequent degradation (20-24). CDK4/6 inhibitors have shown efficacy in hormone receptor-positive breast cancer (49-51), and several MDM2 inhibitors have been developed, with some advancing to clinical trials (52-58). However, CDK4/6 inhibitors (59,60) and MDM2 inhibitors (52-58) have demonstrated only limited activity in WDLPS/DDLPS.

Ferroptosis, a form of necrotic cell death characterized by the oxidative modification of phospholipid membranes through an iron-dependent mechanism (9), has been identified as a potential mechanism of action for various anticancer treatments across multiple cancers (61-65), including sarcomas (66). MDM2, a key oncogene in DDLPS (19), negatively regulates TP53 (20), which itself is a critical regulator of ferroptosis (16-18). Therefore, the investigation of ferroptosis regulation in DDLPS may lead to the identification of new therapeutic strategies for this deadly disease.

GPX4, SLC7A11 and SLC3A2 are three key regulators of ferroptosis resistance. GPX4 dependency has been identified as a unique characteristic of therapy-resistant cancer (67). In the present study, the bioinformatics analysis of publicly available revealed that the expression level of GPX4 in DDLPS is significantly lower compared with that in adipose tissue and WDLPS. *In vitro* experiments revealed that DDLPS cells are highly sensitive to RSL3 and erastin, indicating a susceptibility to ferroptosis. Conversely, SLC7A11 and SLC3A2, two components of xCT, were found to be more highly expressed in LPS than in benign tissue. The upregulation of SLC7A11 may be partially due to the downregulation of TP53 by MDM2 in WDLPS and DDLPS. The mechanism by which TP53 mediates SLC3A2 expression is complex; previous studies have shown that SLC3A2 is upregulated by mutant, but not wild-type, TP53 (68,69). Therefore, further exploration of the regulatory mechanisms of ferroptosis in DDLPS is warranted.

Given that MDM2 is a well-known oncogene in DDLPS, the potential synergistic effect of nutlin-3, a MDM2 inhibitor, with erastin and RSL3 was explored. The treatment sequence was identified as a critical determinant of the efficacy of erastin. Co-treatment with nutlin-3 did not markedly affect the lipid-peroxidation-inducing and cytotoxic effects of erastin. However, treatment with nutlin-3 for 24 h prior to treatment with erastin significantly augmented the induction of lipid-peroxidation and cytotoxicity of erastin in both DDLPS cell lines. This effect of nutlin-3 was not observed with RSL3. These findings suggest that nutlin-3 may sensitize DDLPS cell lines to erastin, potentially by modulating the expression of ferroptosis-related genes underlying its effects.

Immunoblotting revealed that nutlin-3 upregulated SLC3A2 expression in both DDLPS cell lines. Subsequently, nutlin-3 was shown to increase cystine uptake in an erastin-suppressible manner, which may be attributed to SLC3A2 upregulation. Additionally, the nutlin-3-induced expression of SLC3A2 was abolished by TP53 KD. These findings suggest that nutlin-3 treatment induces TP53-mediated SLC3A2 upregulation, leading to increased cystine uptake and erastin sensitivity in DDLPS.

Notably, SLC7A11 expression levels remained largely unchanged after nutlin-3 treatment. TP53, a key suppressor of SLC7A11, is expected to decrease the levels of SLC7A11 when TP53 function is restored (16), as nutlin-3 dissociates MDM2 from TP53, thereby preventing the degradation of TP53 by ubiquitination (38-40). However, as MDM2 is also released and is known to upregulate SLC7A11 (70,71), the enhancing effect of MDM2 on SLC7A11 expression may be counterbalanced by the suppressive effect of restored TP53.

The present study found that treatment with nutlin-3 prior to treatment with erastin or RSL3 increased lipid peroxidation, a hallmark of ferroptosis, and apoptosis. Nutlin-3 alone is known to induce apoptosis via cell cycle arrest or the restoration of TP53 function (72-74). mTOR is crucial in different types of programmed cell death (75), including apoptosis (44-46) and ferroptosis (41-43). In the present study, combining nutlin-3 with either erastin or RSL3 reduced the absolute levels of phosphorylated proteins in the mTOR pathway but not the phosphorylated/total protein ratios, suggesting the potential role of the mTOR pathway in the apoptosis induction of these combinations. Further investigations are needed to confirm this finding.

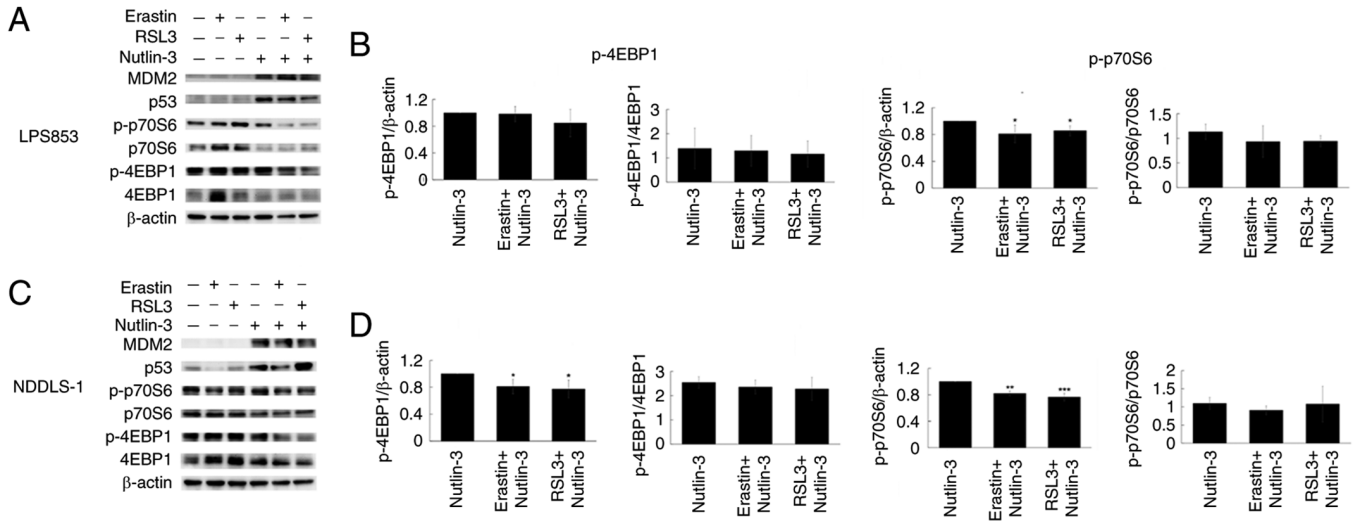

Figure 10. Immunoblotting of mTOR pathway proteins eukaryotic translation initiation factor 4E binding protein 1 (4EBP1) and p70 ribosomal protein S6 kinase (p70S6) in dedifferentiated liposarcoma cell lines following treatment with erastin or RSL3, alone or with nutlin-3 pre-treatment. (A) Representative western blots and (B) quantified levels of phosphorylated proteins in LPS853 cells. (C) Representative western blots and (D) quantified levels of phosphorylated proteins in NDDLS-1 cells. Results are presented as the mean ± standard error of the mean relative to β-actin (left) or total target protein (right), from three independent experiments. *P<0.05, **P<0.01 and ***P<0.001 vs. nutlin-3.

The present bioinformatics analysis revealed that HMGCR expression is upregulated in LPS. However, lovastatin and simvastatin, two inhibitors of HMGCR, showed minimal effects on lipid peroxidation and only modest cytotoxicity against the two DDLPS cell lines, suggesting that the HMGCR pathway may not play a major role in the regulation of ferroptosis in DDLPS. DPP4 expression was also found to be upregulated in LPS, likely due to TP53 downregulation in WDLPS and DDLPS (18). DPP4 is an exoprotease that is expressed by different cell types and plays a role in plasma membrane-associated lipid peroxidation (18). However, previous studies have shown that its role in cancer is primarily restricted to the tumor microenvironment (76). Therefore, these two genes were not pursued further in the present study.

In summary, the present study showed that several ferroptosis-related genes are differentially expressed in DDLPS. Additionally, *in vitro* experiments demonstrated that DDLPS cell lines are highly sensitive to the lipid peroxidation-inducing and cytotoxic effects of erastin and RSL3. Furthermore, pre-treatment with nutlin-3 significantly increased the efficacy of erastin in DDLPS cell lines, potentially via the TP53-mediated upregulation of SLC3A2, resulting in increased cystine uptake and vulnerability to ferroptosis. Suppression of the mTOR pathway may contribute to the apoptosis-inducing effects observed with the nutlin-3-containing combinations. This mechanism may contribute to resistance to MDM2 inhibitors in DDLPS. These findings provide valuable insights into the potential development of novel treatments for DDLPS. In future studies, it is planned to examine the combined effect of MDM2 inhibitors and ferroptosis-inducing agents in greater detail, and to explore the underlying mechanisms in an *in vivo* model.

Acknowledgements

Not applicable.

Funding

This study was jointly supported by grants from the National Science and Technology Council (grant nos. MOST 110-2314-B-075-070 and MOST 111-2314-B-075-022), and Taipei Veterans General Hospital (grant nos. V110D56-002-MY2-1, V110D56-002-MY2-2, V110C-208, V112C-093 and V113C-116). This study was also supported by the Taiwan Clinical Oncology Research Foundation, Melissa Lee Cancer Foundation (grant no. MLCF_V114_A11403), and the Chong Hin Loon Memorial Cancer and Biotherapy Research Center of National Yang Ming Chiao Tung University.

Availability of data and materials

The data generated in the present study may be requested from the corresponding author.

Authors' contributions

CCY, PCHC, TCC and JAF were responsible for the design and conception of the study. MHY, CHY and YCL were responsible for data acquisition. SCC, WCW, PKW, CMC and JYW were responsible for data interpretation. CCY was responsible for writing the original draft of the manuscript. PCHC and JAF reviewed and edited the manuscript. CHY and YCL edited the figures. TCC and MHY confirm the authenticity of all the raw data. All authors read and approved the final version of the manuscript.

Ethics approval and consent to participate

This study was deemed as being exempt from ethical review by the Institutional Review Board (IRB) of Taipei Veterans General Hospital (IRB no. 2021-07-003AE).

Patient consent for publication

Not applicable.

Competing interests

The authors declare that they have no competing interests

Use of artificial intelligence tools

During the preparation of this work, artificial intelligence (AI) tools were used to improve the readability and language of the manuscript, and subsequently, the authors revised and edited the content produced by the AI tools as necessary, taking full responsibility for the ultimate content of the manuscript.

References

1. Hung GY, Yen CC, Horng JL, Liu CY, Chen WM, Chen TH and Liu CL: Incidences of primary soft tissue sarcoma diagnosed on extremities and trunk wall: A population-based study in taiwan. Medicine (Baltimore) 94: e1696, 2015.
2. Hung GY, Horng JL, Chen PC, Lin LY, Chen JY, Chuang PH, Chao TC and Yen CC: Incidence of soft tissue sarcoma in Taiwan: A nationwide population-based study (2007-2013). Cancer Epidemiol 60: 185-192, 2019.
3. Ducimetiere F, Lurkin A, Ranchere-Vince D, Decouvelaere AV, Peoc'h M, Istier L, Chalabreysse P, Muller C, Alberti L, Bringuier PP, *et al*: Incidence of sarcoma histotypes and molecular subtypes in a prospective epidemiological study with central pathology review and molecular testing. PLoS One 6: e20294, 2011.
4. Lee ATJ, Thway K, Huang PH and Jones RL: Clinical and molecular spectrum of liposarcoma. J Clin Oncol 36: 151-159, 2018.
5. Seddon B, Strauss SJ, Whelan J, Leahy M, Woll PJ, Cowie F, Rothermundt C, Wood Z, Benson C, Ali N, *et al*: Gemcitabine and docetaxel versus doxorubicin as first-line treatment in previously untreated advanced unresectable or metastatic soft-tissue sarcomas (GeDDiS): A randomised controlled phase 3 trial. Lancet Oncol 18: 1397-1410, 2017.
6. Schoffski P, Chawla S, Maki RG, Italiano A, Gelderblom H, Choy E, Grignani G, Camargo V, Bauer S, Rha SY, *et al*: Eribulin versus dacarbazine in previously treated patients with advanced liposarcoma or leiomyosarcoma: A randomised, open-label, multicentre, phase 3 trial. Lancet 387: 1629-1637, 2016.
7. Demetri GD, Schoffski P, Grignani G, Blay JY, Maki RG, Van Tine BA, Alcindor T, Jones RL, D'Adamo DR, Guo M and Chawla S: Activity of eribulin in patients with advanced liposarcoma demonstrated in a subgroup analysis from a randomized phase III study of eribulin versus dacarbazine. J Clin Oncol 35: 3433-3439, 2017.
8. Demetri GD, von Mehren M, Jones RL, Hensley ML, Schuetze SM, Staddon A, Milhem M, Elias A, Ganjoo K, Tawbi H, *et al*: Efficacy and safety of trabectedin or dacarbazine for metastatic liposarcoma or leiomyosarcoma after failure of conventional chemotherapy: Results of a phase III randomized multicenter clinical trial. J Clin Oncol 34: 786-793, 2016.
9. Conrad M, Angeli JP, Vandenabeele P and Stockwell BR: Regulated necrosis: Disease relevance and therapeutic opportunities. Nat Rev Drug Discov 15: 348-366, 2016.
10. Xie Y, Hou W, Song X, Yu Y, Huang J, Sun X, Kang R and Tang D: Ferroptosis: Process and function. Cell Death Differ 23: 369-379, 2016.
11. Stockwell BR, Friedmann Angeli JP, Bayir H, Bush AI, Conrad M, Dixon SJ, Fulda S, Gascon S, Hatzios SK, Kagan VE, *et al*: Ferroptosis: A regulated cell death nexus linking metabolism, redox biology, and disease. Cell 171: 273-285, 2017.
12. Ingold I, Berndt C, Schmitt S, Doll S, Poschmann G, Buday K, Roveri A, Peng X, Porto Freitas F, Seibt T, *et al*: Selenium utilization by GPX4 is required to prevent hydroperoxide-induced ferroptosis. Cell 172: 409-422 e421, 2018.
13. Yang WS, SriRamaratnam R, Welsch ME, Shimada K, Skouta R, Viswanathan VS, Cheah JH, Clemons PA, Shamji AF, Clish CB, *et al*: Regulation of ferroptotic cancer cell death by GPX4. Cell 156: 317-331, 2014.
14. Dixon SJ, Lemberg KM, Lamprecht MR, Skouta R, Zaitsev EM, Gleason CE, Patel DN, Bauer AJ, Cantley AM, Yang WS, *et al*: Ferroptosis: An iron-dependent form of nonapoptotic cell death. Cell 149: 1060-1072, 2012.
15. Cheok CF, Verma CS, Baselga J and Lane DP: Translating p53 into the clinic. Nat Rev Clin Oncol 8: 25-37, 2011.
16. Jiang L, Kon N, Li T, Wang SJ, Su T, Hibshoosh H, Baer R and Gu W: Ferroptosis as a p53-mediated activity during tumour suppression. Nature 520: 57-62, 2015.
17. Moon SH, Huang CH, Houlihan SL, Regunath K, Freed-Pastor WA, Morris JP, Tschaharganeh DF, Kastenhuber ER, Barsotti AM, Culp-Hill R, *et al*: p53 represses the mevalonate pathway to mediate tumor suppression. Cell 176: 564-580 e519, 2019.
18. Xie Y, Zhu S, Song X, Sun X, Fan Y, Liu J, Zhong M, Yuan H, Zhang L, Billiar TR, *et al*: The tumor suppressor p53 limits ferroptosis by blocking DPP4 activity. Cell Rep 20: 1692-1704, 2017.
19. Dei Tos AP, Doglioni C, Piccinin S, Sciot R, Furlanetto A, Boiocchi M, Dal CP, Maestro R, Fletcher CD and Tallini G: Coordinated expression and amplification of the MDM2, CDK4, and HMGI-C genes in atypical lipomatous tumours. J Pathol 190: 531-536, 2000.
20. Karni-Schmidt O, Lokshin M and Prives C: The roles of MDM2 and MDMX in cancer. Annu Rev Pathol 11: 617-644, 2016.
21. Leslie PL and Zhang Y: MDM2 oligomers: Antagonizers of the guardian of the genome. Oncogene 35: 6157-6165, 2016.
22. Hock AK and Vousden KH: The role of ubiquitin modification in the regulation of p53. Biochim Biophys Acta 1843: 137-149, 2014.
23. do Patrocinio AB, Rodrigues V and Guidi Magalhaes L: P53: Stability from the ubiquitin-proteasome system and specific 26S proteasome inhibitors. ACS Omega 7: 3836-3843, 2022.
24. Bang S, Kaur S and Kurokawa M: Regulation of the p53 family proteins by the ubiquitin proteasomal pathway. Int J Mol Sci 21: 261, 2019.
25. Venkatesh D, O'Brien NA, Zandkarimi F, Tong DR, Stokes ME, Dunn DE, Kengmana ES, Aron AT, Klein AM, Csuka JM, *et al*: MDM2 and MDMX promote ferroptosis by PPARalpha-mediated lipid remodeling. Genes Dev 34: 526-543, 2020.
26. Yen CC, Chen LT, Li CF, Chen SC, Chua WY, Lin YC, Yen CH, Chen YC, Yang MH, Chao Y and Fletcher JA: Identification of phenothiazine as an ETV1targeting agent in gastrointestinal stromal tumors using the connectivity map. Int J Oncol 55: 536-546, 2019.
27. Chibon F, Lagarde P, Salas S, Perot G, Brouste V, Tirode F, Lucchesi C, de Reynies A, Kauffmann A, Bui B, *et al*: Validated prediction of clinical outcome in sarcomas and multiple types of cancer on the basis of a gene expression signature related to genome complexity. Nat Med 16: 781-787, 2010.
28. Gobble RM, Qin LX, Brill ER, Angeles CV, Ugras S, O'Connor RB, Moraco NH, Decarolis PL, Antonescu C and Singer S: Expression profiling of liposarcoma yields a multigene predictor of patient outcome and identifies genes that contribute to liposarcomagenesis. Cancer Res 71: 2697-2705, 2011.
29. Doyle KR, Mitchell MA, Roberts CL, James S, Johnson JE, Zhou Y, von Mehren M, Lev D, Kipling D and Broccoli D: Validating a gene expression signature proposed to differentiate liposarcomas that use different telomere maintenance mechanisms. Oncogene 31: 265-266; author reply 267-268, 2012.
30. Yoshino J, Conte C, Fontana L, Mittendorfer B, Imai S, Schechtman KB, Gu C, Kunz I, Rossi Fanelli F, Patterson BW and Klein S: Resveratrol supplementation does not improve metabolic function in nonobese women with normal glucose tolerance. Cell Metab 16: 658-664, 2012.
31. Nookaew I, Svensson PA, Jacobson P, Jernas M, Taube M, Larsson I, Andersson-Assarsson JC, Sjostrom L, Froguel P, Walley A, *et al*: Adipose tissue resting energy expenditure and expression of genes involved in mitochondrial function are higher in women than in men. J Clin Endocrinol Metab 98: E370-E378, 2013.
32. Li C and Wong WH: Model-based analysis of oligonucleotide arrays: Model validation, design issues and standard error application. Genome Biol 2: RESEARCH0032, 2001.
33. Li C and Wong WH: Model-based analysis of oligonucleotide arrays: Expression index computation and outlier detection. Proc Natl Acad Sci USA 98: 31-36, 2001.

34. Yoshida Y, Shimakawa S, Itoh N and Niki E: Action of DCFH and BODIPY as a probe for radical oxidation in hydrophilic and lipophilic domain. Free Radic Res 37: 861-872, 2003.
35. Chou TC and Talalay P: Quantitative analysis of dose-effect relationships: The combined effects of multiple drugs or enzyme inhibitors. Adv Enzyme Regul 22: 27-55, 1984.
36. Chou YS, Yen CC, Chen WM, Lin YC, Wen YS, Ke WT, Wang JY, Liu CY, Yang MH, Chen TH and Liu CL: Cytotoxic mechanism of PLK1 inhibitor GSK461364 against osteosarcoma: Mitotic arrest, apoptosis, cellular senescence, and synergistic effect with paclitaxel. Int J Oncol 48: 1187-1194, 2016.
37. Livak KJ and Schmittgen TD: Analysis of relative gene expression data using real-time quantitative PCR and the 2(-Delta Delta C(T)) method. Methods 25: 402-408, 2001.
38. Vassilev LT, Vu BT, Graves B, Carvajal D, Podlaski F, Filipovic Z, Kong N, Kammlott U, Lukacs C, Klein C, *et al*: In vivo activation of the p53 pathway by small-molecule antagonists of MDM2. Science 303: 844-848, 2004.
39. Tovar C, Rosinski J, Filipovic Z, Higgins B, Kolinsky K, Hilton H, Zhao X, Vu BT, Qing W, Packman K, *et al*: Small-molecule MDM2 antagonists reveal aberrant p53 signaling in cancer: Implications for therapy. Proc NatI Acad Sci USA 103: 1888-1893, 2006.
40. Henze J, Muhlenberg T, Simon S, Grabellus F, Rubin B, Taeger G, Schuler M, Treckmann J, Debiec-Rychter M, Taguchi T, *et al*: p53 modulation as a therapeutic strategy in gastrointestinal stromal tumors. PLoS One 7: e37776, 2012.
41. Shi Z, Naowarojna N, Pan Z and Zou Y: Multifaceted mechanisms mediating cystine starvation-induced ferroptosis. Nat Commun 12: 4792, 2021.
42. Wang Z, Zong H, Liu W, Lin W, Sun A, Ding Z, Chen X, Wan X, Liu Y, Hu Z, *et al*: Augmented ERO1alpha upon mTORC1 activation induces ferroptosis resistance and tumor progression via upregulation of SLC7A11. J Exp Clin Cancer Res 43: 112, 2024.
43. Yin J, Chen J, Hong JH, Huang Y, Xiao R, Liu S, Deng P, Sun Y, Chai KXY, Zeng X, *et al*: 4EBP1-mediated SLC7A11 protein synthesis restrains ferroptosis triggered by MEK inhibitors in advanced ovarian cancer. JCI Insight 9: e177857, 2024.
44. Han J, Wang L, Lv H, Liu J, Dong Y, Shi L and Ji Q: EphA2 inhibits SRA01/04 cells apoptosis by suppressing autophagy via activating PI3K/Akt/mTOR pathway. Arch Biochem Biophys 711: 109024, 2021.
45. Yang J, Pi C and Wang G: Inhibition of PI3K/Akt/mTOR pathway by apigenin induces apoptosis and autophagy in hepatocellular carcinoma cells. Biomed Pharmacother 103: 699-707, 2018.
46. Li W, Li D, Ma Q, Chen Y, Hu Z, Bai Y and Xie L: Targeted inhibition of mTOR by BML-275 induces mitochondrial-mediated apoptosis and autophagy in prostate cancer. Eur J Pharmacol 957: 176035, 2023.
47. Fletcher CD: The evolving classification of soft tissue tumours-An update based on the new 2013 WHO classification. Histopathology 64: 2-11, 2014.
48. Sherr CJ, Beach D and Shapiro GI: Targeting CDK4 and CDK6: From discovery to therapy. Cancer Discov 6: 353-367, 2016.
49. Finn RS, Martin M, Rugo HS, Jones S, Im SA, Gelmon K, Harbeck N, Lipatov ON, Walshe JM, Moulder S, *et al*: Palbociclib and letrozole in advanced breast cancer. N Engl J Med 375: 1925-1936, 2016.
50. Hortobagyi GN, Stemmer SM, Burris HA, Yap YS, Sonke GS, Paluch-Shimon S, Campone M, Petrakova K, Blackwell KL, Winer EP, *et al*: Updated results from MONALEESA-2, a phase III trial of first-line ribociclib plus letrozole versus placebo plus letrozole in hormone receptor-positive, HER2-negative advanced breast cancer. Ann Oncol 29: 1541-1547, 2018.
51. Goetz MP, Toi M, Campone M, Sohn J, Paluch-Shimon S, Huober J, Park IH, Tredan O, Chen SC, Manso L, *et al*: MONARCH 3: Abemaciclib as initial therapy for advanced breast cancer. J Clin Oncol 35: 3638-3646, 2017.
52. Wang S, Zhao Y, Aguilar A, Bernard D and Yang CY: Targeting the MDM2-p53 protein-protein interaction for new cancer therapy: Progress and challenges. Cold Spring Harb Perspect Med 7: a026245, 2017.
53. Kocik J, Machula M, Wisniewska A, Surmiak E, Holak TA and Skalniak L: Helping the released guardian: Drug combinations for supporting the anticancer activity of HDM2 (MDM2) antagonists. Cancers (Basel) 11: 1014, 2019.
54. Fang Y, Liao G and Yu B: Small-molecule MDM2/X inhibitors and PROTAC degraders for cancer therapy: Advances and perspectives. Acta Pharm Sin B 10: 1253-1278, 2020.
55. Zhao Y, Aguilar A, Bernard D and Wang S: Small-molecule inhibitors of the MDM2-p53 protein-protein interaction (MDM2 Inhibitors) in clinical trials for cancer treatment. J Med Chem 58: 1038-1052, 2015.
56. LoRusso P, Yamamoto N, Patel MR, Laurie SA, Bauer TM, Geng J, Davenport T, Teufel M, Li J, Lahmar M and Gounder MM: The MDM2-p53 Antagonist brigimadlin (BI 907828) in patients with advanced or metastatic solid tumors: Results of a phase Ia, first-in-human, dose-escalation study. Cancer Discov 13: 1802-1813, 2023.
57. Ray-Coquard I, Blay JY, Italiano A, Le Cesne A, Penel N, Zhi J, Heil F, Rueger R, Graves B, Ding M, *et al*: Effect of the MDM2 antagonist RG7112 on the P53 pathway in patients with MDM2-amplified, well-differentiated or dedifferentiated liposarcoma: An exploratory proof-of-mechanism study. Lancet Oncol 13: 1133-1140, 2012.
58. Gounder MM, Bauer TM, Schwartz GK, Weise AM, LoRusso P, Kumar P, Tao B, Hong Y, Patel P, Lu Y, *et al*: A first-in-human Phase I study of milademetan, an MDM2 inhibitor, in patients with advanced liposarcoma, solid tumors, or lymphomas. J Clin Oncol 41: 1714-1724, 2023.
59. Assi T, Kattan J, Rassy E, Nassereddine H, Farhat F, Honore C, Le Cesne A, Adam J and Mir O: Targeting CDK4 (cyclin-dependent kinase) amplification in liposarcoma: A comprehensive review. Crit Rev Oncol Hematol 153: 103029, 2020.
60. Dickson MA, Schwartz GK, Keohan ML, D'Angelo SP, Gounder MM, Chi P, Antonescu CR, Landa J, Qin LX, Crago AM, *et al*: Progression-free survival among patients with well-differentiated or dedifferentiated liposarcoma treated with CDK4 inhibitor palbociclib: A phase 2 Clinical Trial. JAMA Oncol 2: 937-940, 2016.
61. Guo J, Xu B, Han Q, Zhou H, Xia Y, Gong C, Dai X, Li Z and Wu G: Ferroptosis: A novel anti-tumor action for cisplatin. Cancer Res Treat 50: 445-460, 2018.
62. Ma S, Henson ES, Chen Y and Gibson SB: Ferroptosis is induced following siramesine and lapatinib treatment of breast cancer cells. Cell Death Dis 7: e2307, 2016.
63. Trujillo-Alonso V, Pratt EC, Zong H, Lara-Martinez A, Kaittanis C, Rabie MO, Longo V, Becker MW, Roboz GJ, Grimm J and Guzman ML: FDA-approved ferumoxytol displays anti-leukaemia efficacy against cells with low ferroportin levels. Nat Nanotechnol 14: 616-622, 2019.
64. Yamaguchi Y, Kasukabe T and Kumakura S: Piperlongumine rapidly induces the death of human pancreatic cancer cells mainly through the induction of ferroptosis. Int J Oncol 52: 1011-1022, 2018.
65. Sun X, Ou Z, Chen R, Niu X, Chen D, Kang R and Tang D: Activation of the p62-Keap1-NRF2 pathway protects against ferroptosis in hepatocellular carcinoma cells. Hepatology 63: 173-184, 2016.
66. Brashears CB, Prudner BC, Rathore R, Caldwell KE, Dehner CA, Buchanan JL, Lange SES, Poulin N, Sehn JK, Roszik J, *et al*: Malic enzyme 1 absence in synovial sarcoma shifts antioxidant system dependence and increases sensitivity to ferroptosis induction with ACXT-3102. Clin Cancer Res 28: 3573-3589, 2022.
67. Viswanathan VS, Ryan MJ, Dhruv HD, Gill S, Eichhoff OM, Seashore-Ludlow B, Kaffenberger SD, Eaton JK, Shimada K, Aguirre AJ, *et al*: Dependency of a therapy-resistant state of cancer cells on a lipid peroxidase pathway. Nature 547: 453-457, 2017.
68. Mello SS, Valente LJ, Raj N, Seoane JA, Flowers BM, McClendon J, Bieging-Rolett KT, Lee J, Ivanochko D, Kozak MM, *et al*: A p53 super-tumor suppressor reveals a tumor suppressive p53-ptpn14-yap axis in pancreatic cancer. Cancer Cell 32: 460-473, 2017.
69. Tombari C, Zannini A, Bertolio R, Pedretti S, Audano M, Triboli L, Cancila V, Vacca D, Caputo M, Donzelli S, *et al*: Mutant p53 sustains serine-glycine synthesis and essential amino acids intake promoting breast cancer growth. Nat Commun 14: 6777, 2023.
70. Fujihara KM, Corrales Benitez M, Cabalag CS, Zhang BZ, Ko HS, Liu DS, Simpson KJ, Haupt Y, Lipton L, Haupt S, *et al*: SLC7A11 Is a superior determinant of APR-246 (Eprenetapopt) response than TP53 mutation status. Mol Cancer Ther 20: 1858-1867, 2021.
71. Riscal R, Schrepfer E, Arena G, Cisse MY, Bellvert F, Heuillet M, Rambow F, Bonneil E, Sabourdy F, Vincent C, *et al*: Chromatin-bound MDM2 regulates serine metabolism and redox homeostasis independently of p53. Mol Cell 62: 890-902, 2016.

72. Villalonga-Planells R, Coll-Mulet L, Martinez-Soler F, Castano E, Acebes JJ, Gimenez-Bonafe P, Gil J and Tortosa A: Activation of p53 by nutlin-3a induces apoptosis and cellular senescence in human glioblastoma multiforme. PLoS One 6: e18588, 2011.
73. Miyachi M, Kakazu N, Yagyu S, Katsumi Y, Tsubai-Shimizu S, Kikuchi K, Tsuchiya K, Iehara T and Hosoi H: Restoration of p53 pathway by nutlin-3 induces cell cycle arrest and apoptosis in human rhabdomyosarcoma cells. Clin Cancer Res 15: 4077-4084, 2009.
74. Manfe V, Biskup E, Johansen P, Kamstrup MR, Krejsgaard TF, Morling N, Wulf HC and Gniadecki R: MDM2 inhibitor nutlin-3a induces apoptosis and senescence in cutaneous T-cell lymphoma: role of p53. J Invest Dermatol 132: 1487-1496, 2012.
75. Xie Y, Lei X, Zhao G, Guo R and Cui N: mTOR in programmed cell death and its therapeutic implications. Cytokine Growth Factor Rev 71-72: 66-81, 2023.
76. Cordero OJ: CD26 and cancer. Cancers (Basel) 14: 5194, 2022.